Inorganic Chemistry

Article

pubs.acs.org/IC

A Layered Mixed Zirconium Phosphate/Phosphonate with Exposed Carboxylic and Phosphonic Groups: X-ray Powder Structure and Proton Conductivity Properties

Anna Donnadio,[†] Morena Nocchetti,[‡] Ferdinando Costantino,[†] Marco Taddei,[†] Mario Casciola,[†] Fábio da Silva Lisboa,[§] and Riccardo Vivani*[,‡]

[†]Dipartimento di Chimica, Biologia e Biotecnologie, Università di Perugia, Via Elce di Sotto, 8, 06123 Perugia, Italy

[‡]Dipartimento di Scienze Farmaceutiche, Università di Perugia, Via del Liceo 1, 06123 Perugia, Italy

[§]Departamento de Química, Universidade Federal do Paraná, Jardim das Américas CEP − 81.531-980, 19032 Curitiba, Brasil

Supporting Information

ABSTRACT: A novel mixed zirconium phosphate/phosphonate based on glyphosine, of formula $Zr_2(PO_4)H_5(L)_2{\cdot}H_2O$ [L = $(O_3PCH_2)_2NCH_2COO$], was synthesized in mild conditions. The compound has a layered structure that was solved *ab initio* from laboratory PXRD data. It crystallizes in the monoclinic $C2/c$ space group with the following cell parameters: a = 29.925(3), b = 8.4225(5), c = 9.0985(4) Å, and β = 98.474(6)°. Phosphate groups are placed inside the sheets and connect the zirconium atoms in a tetradentate fashion, while uncoordinated carboxylate and P−OH phosphonate groups are exposed on the layer surface. Due to the presence of these acidic groups, the compound showed remarkable proton conductivity properties, which were studied in a wide range of temperature and relative humidity (RH). The conductivity is strongly dependent on RH and reaches 1×10^{-3} S cm^{-1} at 140 °C and 95% RH. At this RH, the activation energy of conduction is 0.15 eV in the temperature range 80−140 °C. The similarities of this structure with related structures already reported in the literature were also discussed.

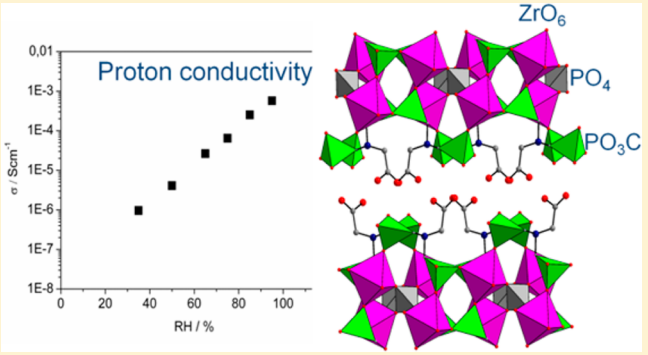

INTRODUCTION

Zirconium phosphonates are a class of materials characterized by high insolubility and good ion exchange and intercalation properties. These features make them suitable in many fields of current interest such as fillers for polymeric nanocomposites, molecular recognition, separation, and so on.[1] They have also been studied for their good proton conductivity properties in a wide range of relative humidity and temperature.[2] This property is frequently accompanied by a remarkable chemical and thermal stability. These joint features are intriguing owing to the potential application of these materials in a variety of devices, including fuel cells, electrolyzers, chemical sensors, electrochromic displays, hydrogen pumps, and so on.[3] In this respect, the proton conductivity properties of a high number of hybrid crystalline materials like coordination polymers and metal−organic frameworks have been reported in the past few years, many of which are metal phosphonates.[4] Recently, we reported on the preparation and characterization of a novel layered zirconium phosphonate based on N,N-bis-(phosphonomethyl)glycine (glyphosine), a simple carboxy-amino diphosphonate (Chart 1).[5]

In this compound, due to the unusually high value of the P/Zr molar ratio (8/3), half of the phosphonate groups coordinate three zirconium atoms, while the other half is bidentate. The uncoordinated oxygen atom points toward the interlayer region, forming a network of polar interactions with carboxylic groups and hydration water molecules.

This compound showed a good proton conductivity, which reached the highest value (about 8×10^{-4} S cm^{-1}) at 140 °C and 95% relative humidity (RH), which can be related to the presence of these uncoordinated polar groups with different acidity.

Chart 1. Molecular Structures of Glyphosine and PMIDA

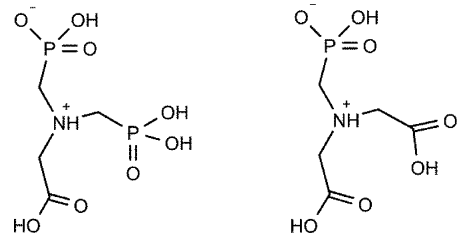

Received: October 9, 2014
Published: November 26, 2014

   dx.doi.org/10.1021/ic502473w | *Inorg. Chem.* 2014, 53, 13220−13226

In mid-1990s, Clearfield and co-workers explored the reactivity of a phosphonic building block, N,N-phosphonomethylimino-diacetic acid (PMIDA), that has a molecular geometry similar to that of glyphosine (Chart 1). They found that zirconium is able to form a 1D structure when reacting exclusively with PMIDA and a layered structure when phosphoric acid is added to the reaction solution (ZPPMIDA). In the latter, zirconium is coordinated with both phosphate and PMIDA, and the interlayer region accommodates the two carboxylate groups (Figure 1).[6]

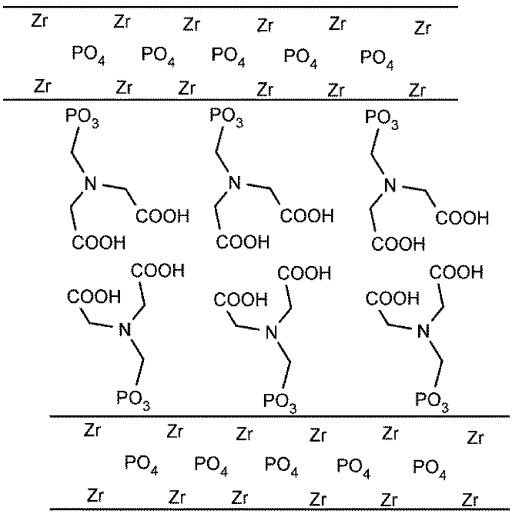

Figure 1. Schematic representation of the structure of ZPPMIDA.

The similarity of glyphosine molecular structure with PMIDA suggested to us to further investigate the zirconium−glyphosine system, also adding phosphoric acid, in the hope to obtain, in analogy to ZPPMIDA, a solid structure containing a considerable number of free acidic phosphonate and carboxylate groups in the interlayer region, which could effectively contribute to the protonic conduction.

As a result of this investigation, a novel microcrystalline compound, built from glyphosine and phosphate was synthesized. Its structure was solved *ab initio* from powder X-ray diffraction (PXRD) data, showing that although it is related with that of ZPPMIDA and rich in uncoordinated carboxylate and phosphonate groups our expectations were not totally complied. However, due to its structure, the obtained material showed increased proton conductivity properties as compared with the parent zirconium−glyphosine derivative.

EXPERIMENTAL SECTION

Chemicals. All of the chemicals were purchased from Sigma-Aldrich and were used as received.

Synthesis of *N,N*-Bis(phosphonomethyl)glycine (Glyphosine). Glyphosine was prepared following the Moedritzer-Irani method;[7] 5 g of glycine (67 mmol) were dissolved in 50 mL of 6 M HCl, together with 11 g of H_3PO_3 (133 mmol). This mixture was heated to reflux, and 8 g of paraformaldehyde (266 mmol) dispersed in 10 mL of water were slowly added within 2 h. After the last addition of paraformaldehyde, the solution was refluxed for 1 more hour and then the solvent was evaporated. The raw mixture was treated with 2-propanol, yielding a white solid that was filtered under vacuum and dried in an oven at 60 °C; 13.6 g of glyphosine was recovered. (Yield = 74%). ^{1}H NMR (D_2O, 400 MHz): δ = 4.29 (singlet, 2H), 3.55 (doublet, J = 6.0 Hz, 4H) ppm. ^{31}P NMR ($CDCl_3$, 400 MHz): δ = 8.13 ppm.

Synthesis of $Zr_2(PO_4)[(HO_3PCH_2)(O_3PCH_2)NHCH_2COOH]$-$[(O_3PCH_2)_2NHCH_2COOH]\cdot H_2O$ (ZPGly). A total of 2.37 g (9 mmol) of glyphosine was solubilized in 93 mL of deionized water, and then 6 mL of 1 M phosphoric acid was added to this solution. A total of 1.93 g (6 mmol) of zirconium oxychloride octahydrate was dissolved in 20.4 mL of 2.9 M hydrofluoric acid solution (59 mmol, HF/Zr^{4+} molar ratio = 10). These two solutions were mixed in a 500 mL Teflon bottle and placed in an oven at 90 °C. After 3 days, the solid was filtered under vacuum, washed three times with deionized water, and dried at 60 °C for 24 h (Yield: 37%). The anhydrous form of ZPGly (hereafter ZPGly-a) was obtained by heating ZPGly at 100 °C. Anal. calc. for $Zr_2P_5O_{21}C_8N_2H_{19}$: Zr 22.3, P 19.4, C 11.7, N 3.4, H 2.3%. Found Zr 23.1, P 18.5, C 10.4, N 3.0, H 2.2%. Quantitative ^{31}P NMR (D_2O/HF, 400 MHz): δ = 8.50 ppm (glyphosine, 4P), 1.07 ppm (phosphoric acid, 1P).

Analytical Procedures. Zirconium and phosphorus contents of samples were obtained by inductively coupled plasma−optical emission spectrophotometry (ICP−OES) using a Varian Liberty Series II instrument working in axial geometry after the mineralization of samples with hydrofluoric acid. Carbon, nitrogen, and hydrogen contents were determined by elemental analysis using an EA 1108 CHN Fisons instrument. PXRD patterns for structure determination and Rietveld refinements were collected with Cu Kα radiation on a PANalytical X'PERT PRO diffractometer and PW3050 goniometer equipped with an X'Celerator detector. The long fine focus (LFF) ceramic tube was operated at 40 kV and 40 mA. To minimize preferential orientations of the microcrystals, the samples were carefully side-loaded onto an aluminum sample holder. The sample was kept at 100 °C by means of a custom-made Peltier equipped sample holder during the data collection. Thermogravimetric (TG) measurements were performed using a Netzsch STA490C thermoanalyser under a 20 mL min^{-1} air flux with a heating rate of 5 °C min^{-1}. Field emission-scanning electron microscopy (FE-SEM) images were collected with a LEO 1525 ZEISS instrument working with an acceleration voltage of 15 kV. Transmittance mid-Fourier transform infrared (FT-IR) measurements were carried out with a JASCO FT/IR 4000 spectrophotometer. The spectral range collected was 400 to 4000 cm^{-1}, with a spectral resolution of 2 cm^{-1} acquiring 100 scans. The samples were dispersed on anhydrous KBr pellets.

Conductivity measurements were carried out on pellets of pressed powder by impedance spectroscopy with a Solartron Sl 1260 impedance/gain phase analyzer in the frequency range of 10 Hz−1 MHz at a signal amplitude of ≤100 mV. Pellets, 10 mm in diameter and 1−1.5 mm thick, were prepared by pressing ∼200 mg of material at 40 kN/cm^2. The two flat surfaces of the pellet were coated with a thin layer of pressed platinum black (Aldrich) mixed with the powder in a 3:1 ratio. RH was controlled by using stainless steel sealed-off cells consisting of two communicating cylindrical compartments held at different temperatures. The cold compartment contained water, while the hot compartment housed the pellet under test. RH values were calculated from the ratio between the pressures of saturated water vapor (p) at the temperatures of the cold (T_c) and hot (T_h) compartment: RH = $p(T_c)/p(T_h) \times 100$.

Water uptake (WU) at controlled temperature and RH was determined as described in ref 5. Specifically, the cell for water uptake had the same size and shape as the conductivity cell and differed from that mainly because the MEA holder is replaced by a glass container hosting the sample (≈ 0.2 g). The cell was equipped with a device that allowed the sample container to be closed with a Teflon plug without opening the cell. After a suitable equilibration time (usually 1 day) at the desired temperature and RH, the sample container was closed, extracted from the cell, and weighed. The water content was determined on the basis of the weight of the material dried at 120 °C for 5 h, taking into account the amount of water trapped in the sample container at the temperature and RH of the experiment. The error on the determination of WU was estimated to be ±0.2 water molecules per unit formula.

Structure Determination and Refinement for ZPGly-a. The crystal structure of ZPGly-a was solved *ab initio* from PXRD data. Indexing was performed using both the TREOR and the DICVOL06

dx.doi.org/10.1021/ic502473w | Inorg. Chem. 2014, 53, 13220−13226

programs.[8] Space group was assigned using the CHEKCELL program.[9] A reliable structural model was determined using the real space global optimization methods implemented in the FOX program. Trial structures were generated using the parallel tempering algorithm. Rietveld refinement of the structural model was performed using the GSAS program.[10] First, zero-shift, cell, background, and profile shape parameters were refined. A corrected pseudo-Voigt profile function (six terms) with two terms for the correction of asymmetry at the low-angle region was used. Then, atomic coordinates were refined by restraining the bond distances to the following values: Zr−O = 2.05(5) Å, P−O = 1.56(5) Å, C−C = 1.54(5) Å, and C−N = 1.45(5) Å. The statistical weight of these restraints was decreased as the refinement proceeded. At the end of the refinement procedure, the shifts in all parameters were less than their standard deviations.

Table 1 reports the crystallographic data and refinement details for ZPGly-a. Figure 2 shows the Rietveld plot for ZPGly-a.

Table 1. Structural Data and Refinement Details for ZPGly-a

compound	ZPGly-a
empirical formula	C_8 N_2 O_{20} P_5 Zr_2
formula weight	781.4
crystal system	Monoclinic
space group	$C2/c$
a (Å)	29.925(3)
b (Å)	8.4225(5)
c (Å)	9.0985(4)
α (deg)	90
β (deg)	98.474(6)
γ (deg)	90
volume (Å)	2268.2(3)
Z	4
T (°C)	100
calculated density (g cm^{-3})	2.29
data range (2θ deg^{-1})	3−100
wavelength (Å)	1.54056
no. of data points	5705
reflections collected, unique	1157
no. of parameters	85
no. of restraints	58
R_p [a]	0.0458
R_{wp} [b]	0.0619
R_F2 [c]	0.0815
GOF[d]	2.67

[a] $R_p = \sum|I_o-I_c|/\sum I_o$. [b] $R_{wp} = [\sum w(I_o-I_c)^2/\sum wI_o^2]^{1/2}$. [c] $R_F2 = \sum|F_o^2 - F_c^2|/\sum|F_o^2|$. [d] GOF $= [\sum w(I_o-I_c)^2/(N_o - N_{var.})]^{1/2}$.

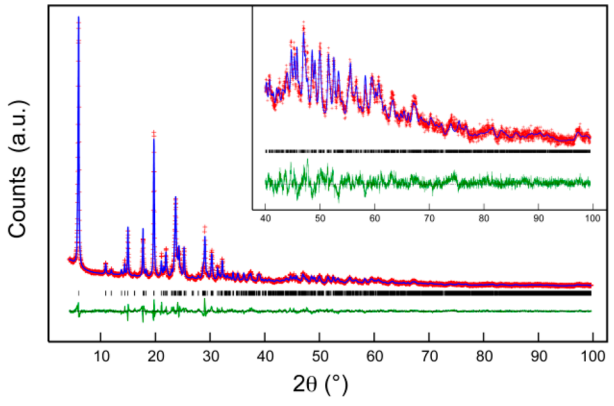

Figure 2. Rietveld plot of ZPGly-a. Inset shows an enlargement of the 40−100° 2θ region.

RESULTS AND DISCUSSION

Structure Description. ZPGly-a crystallizes into the monoclinic $C2/c$ space group, and its structure is composed of the packing of complex hybrid layers along the a-axis. These layers are built from the connection of ZrO_6 octahedra, PO_4 tetrahedra, and PO_3C phosphonate tetrahedra belonging to the glyphosine ligands. The unit cell contains two stacked layers with an ABA sequence. A polyhedral representation and asymmetric unit of ZPGly-a are depicted in Figure 3.

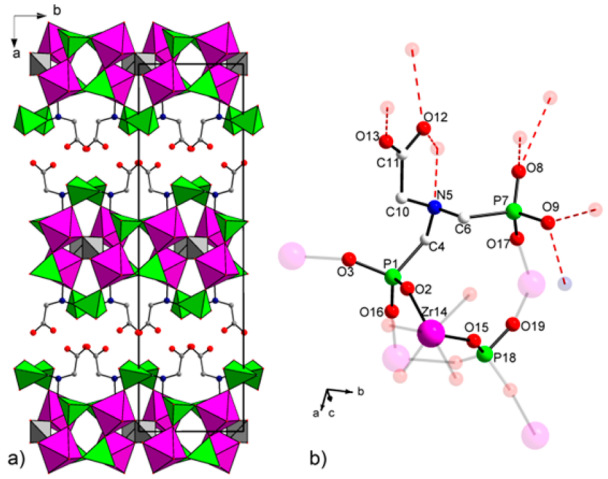

Figure 3. (a) Polyhedral representation of ZPGly-a viewed along the c-axis. ZrO_6 octahedra are in purple. PO_4 tetrahedra are in gray. PO_3C tetrahedra are in green. (b) Asymmetric unit of ZPGly-a. Extended connectivity is represented in light color. Hydrogen bonds are represented as dashed lines.

Each layer is about 15 Å thick. The structure of each layer is constituted of a double plane of ZrO_6 octahedra, which are connected by tetradentate PO_4 groups lying in an intermediate plane. Tetrahedra and octahedra are connected by sharing their vertices. Phosphate groups are placed in special positions inside the layer and link four different zirconium atoms. The glyphosine moieties are placed on the external part of the layers, connecting the zirconium atoms through the PO_3C groups. One PO_3C tetrahedron (P1) is placed inside the ZrO_6 sheet, and it is triply connected to three crystallographically equivalent zirconium octahedra, generating eight-membered $[O-P-O-Zr]_2$ square rings that have been frequently found in other similar zirconium phosphonates.[11] The distances Zr(14)−O(2) and Zr(14)−O(16) are identical [2.08(1) Å], and they are comparable to those found in similar systems. The second PO_3C tetrahedron (P2) is connected to only one Zr atom in a monodentate fashion, with the free P−O groups pointing toward the interlayer space where the organic residue also resides. Thus, a very polar interlayer region in which free carboxylic, P−O, and amino groups are facing each other is found. A number of close contacts between these groups is observed, suggesting that a hydrogen-bond network, extended both inside each layer and between adjacent layers, may be present, as depicted in Figure 4. One P−O group interacts with the oxygen atoms of neighboring carboxylates (P7−O8···O13#1 = 2.99(3) Å, #1 = 0.5 − x, 0.5 − y, 1 − z; P7−O8···O12#2 = 2.73(2) Å, #2 = 0.5 + x, 0.5 − y, 0.5 + z), while the remaining phosphonate oxygen (O9) points toward O12 (P7−O9···O12#3 = 2.58 Å, #3 = x, 1 − y, 0.5 + z) and the aminic nitrogen atom belonging to the adjacent glyphosine moiety

dx.doi.org/10.1021/ic502473w | Inorg. Chem. 2014, 53, 13220−13226

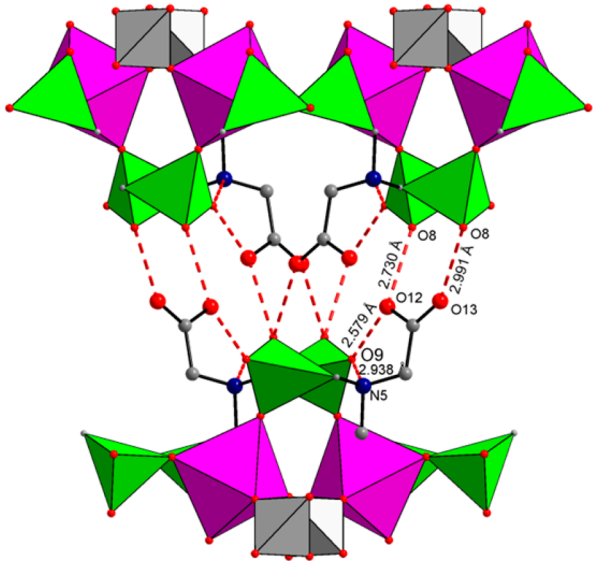

Figure 4. Detail of the H-bond interactions (represented as red dashed lines) between the sheets of ZPGly-a. ZrO_6 octahedra are in purple. PO_4 tetrahedra are in gray. PO_3C tetrahedra are in green.

(P7−O9···N5#3 = 2.94(2) Å). This last interaction was frequently found in many other zirconium aminophosphonates.[12] Very likely the proton resides on the nitrogen atom, as suggested by FT-IR analysis, discussed herein. FT-IR analysis also shows that the carboxylic groups are protonated. For electroneutrality requirements, the P−O8 bond is in turn a double bond and a single bond with protonated oxygen; for best describing this situation, a less symmetrical space group could have been used, such as $P2_1/c$, in order to work with an asymmetric unit containing two distinct glyphosine moieties. However, in all our attempts, the use of this space group did not lead to any improvement of the structure refinement, at the cost of a larger asymmetric unit. Therefore, as $C2/c$ was found to be the largely best fitting space group, we chose to perform structure solution and refinement in this space group.

On the basis of the almost identical PXRD patterns, we can argue that the structure of the as-synthesized ZPGly is very similar to that of ZPGly-a (Figure 1S, Supporting Information), but we were not able to identify the position of the water molecule by difference Fourier maps. This is likely due to the fact that there is only one-half water molecule per asymmetric unit, probably disordered in different positions.

The connectivity of the different building blocks of ZPGly-a is related to that of ZPPMIDA (Figure 5).

In both of them, the PO_4 groups and tridentate PO_3C tetrahedra play the same structural role, However, ZPGly has a higher P/Zr ratio than ZPPMIDA (2.5 vs 1.5) because ZPGly has an additional phosphonate tetrahedron due to the use of the diphosphonic glyphosine instead of the monophosphonic PMIDA moieties. The second phosphonate tetrahedron of glyphosine, being monodentate, replaces the apical water molecule coordinated to zirconium in ZPPMIDA. Therefore, this phosphonate group, although not totally protruding into the interlayer region, as observed for the carboxylates in ZPPMIDA, has two of the three P−O groups that are uncoordinated and free to participate in the building of the highly polar interlayer region.

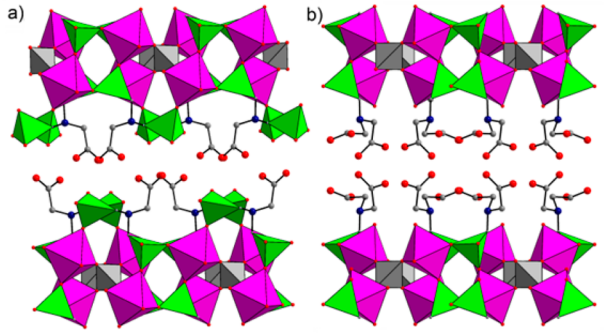

Figure 5. Comparison between the structures of ZPGly-a (a) and ZPPMIDA (b), see ref 12. ZrO_6 octahedra are in purple. PO_4 tetrahedra are in gray. PO_3C tetrahedra are in green.

Thermal Behavior. Figure 6 shows the TG and DTA curves for ZPGly equilibrated over saturated NaCl solution (75% RH).

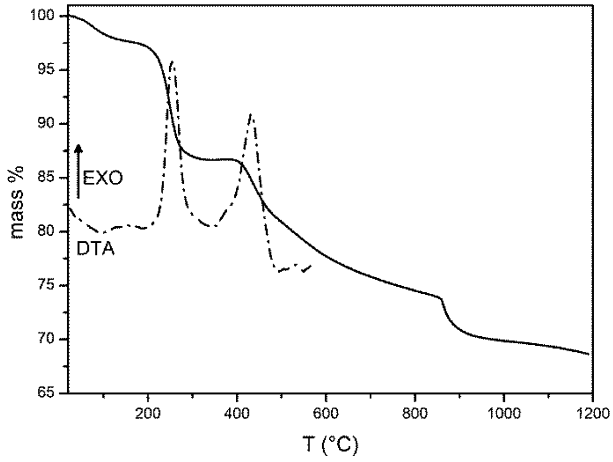

Figure 6. TG and DTA curves of ZPGly conditioned at 75% RH.

The first endothermic weight loss (2.2%) is associated with the loss of one water molecule per formula unit (calculated: 2.2%). The second exothermic weight loss (11.1%), occurring between 150 and 350 °C, corresponds to the loss of two CO_2 molecules per formula unit due to the decarboxylation of the glycine moieties (calculated: 11.0%). The following exothermic step (13.0%), between 350 and 860 °C, is due to the combustion of the organic part to yield ZrP_2O_7 and P_2O_5. The last weight loss can be attributed to the gradual loss of excess P_2O_5. Finally, the solid recovered from the TG was characterized by PXRD, and only cubic ZrP_2O_7 was detected.

FT-IR. The FT-IR spectrum of ZPGly is shown in Figure 7.

At 3424 cm^{-1}, a broad band due to the O−H bond stretching in water is observed, due to the water molecules present in the interlayer space. At 1640 cm^{-1}, the O−H bending of water is also visible. The bands at 3002 and 2995 cm^{-1} are due to the C−H stretching. The broad band centered at 2600 cm^{-1} is typical of a $R_3{-}NH^+$ group, evidencing the presence of protonated amino groups. The band at 1739 cm^{-1} is related to the C═O stretching in a −COOH group, accompanied by the bands at 1427 (O−H bending) and 1244 cm^{-1} (C−O stretching), further evidence of the presence of protonated −COOH groups. The bands from 950 to 1200 cm^{-1} are related to the P−O stretchings, whereas in the region below 900 cm^{-1},

dx.doi.org/10.1021/ic502473w | Inorg. Chem. 2014, 53, 13220−13226

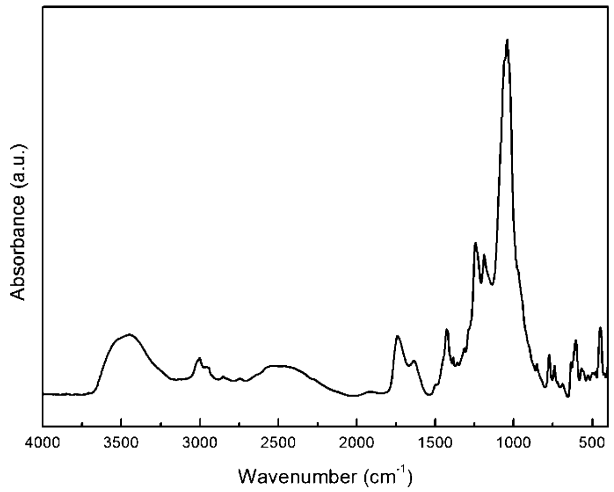

Figure 7. FT-IR spectrum of ZPGly-a.

a number of bands are found, which are not straightforward to be assigned (various bending modes, Zr−O stretchings).

Proton Conductivity. In the unit formula of ZPGly, there are five protogenic functions including R−NH^+ and the hydroxyls belonging to carboxylic and monodentate phosphonic groups. ZPGly is therefore expected to conduct protons, and the conductivity of ZPGly pellets was investigated by complex impedance ($Z^* = Z' + iZ''$) measurements both as a function of temperature at constant RH and as a function of RH at constant temperature. At low RH values, the Nyquist plot (Z'' versus Z') consists in a single depressed semicircle, representing the frequency response of the pellet, followed by a linear region on the low frequency side associated with the electrode−pellet interface (Figure 2S, Supporting Information). With increasing RH, the decrease in the pellet resistance results in a progressive shift of the points of the Nyquist plot from the semicircle to the linear region so that the arc disappears at the highest RH values. In all cases, the pellet conductivity (σ) is calculated from the extrapolation (R) of the linear region to the Z' axis, taking into account the thickness (d) and the flat surface area (A) of the pellet: $\sigma = d/(A \times R)$. The PXRD patterns of the material collected before and after the conductivity measurements did not show significant differences (Figure 3S, Supporting Information), thus indicating that no irreversible transformations take place during the conductivity tests. Measurements at 95% RH were carried out by decreasing temperature from 140 to 80 °C; concomitantly, the water uptake was determined on separate ZPGly pellets under the same experimental conditions. The conductivity decreased from 1×10^{-3} to 5×10^{-4} S cm^{-1} (Figure 8), while the hydration degree was three water molecules per unit formula in the whole temperature range.

As a consequence, the change in conductivity reflects the only change in temperature. This allows us to calculate the activation energy (E_a) of proton conduction on the basis of the Arrhenius equation: $\sigma T = \sigma_0 \exp(-E_a/kT)$, where σ_0 is a temperature independent pre-exponential factor, and k and T have their usual meaning. The E_a value, determined from a least-squares fit of $\log(\sigma T)$ as a function of $1/T$ (Figure 4S, Supporting Information), turns out to be 0.15 eV and is typical of a transport mechanism of the Grotthuss type, which is characterized by E_a values in the range of 0.1−0.4 eV.[2j] The

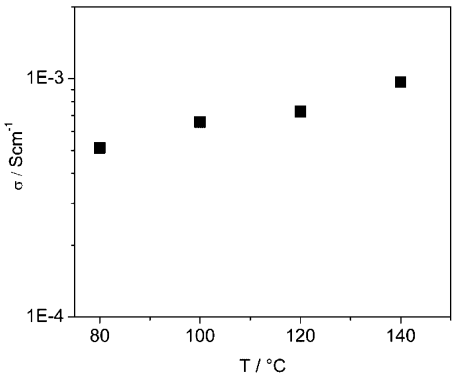

Figure 8. Conductivity of a ZPGly pellet as a function of temperature at 95% RH.

conductivity dependence on RH at 100 °C is shown in Figure 9.

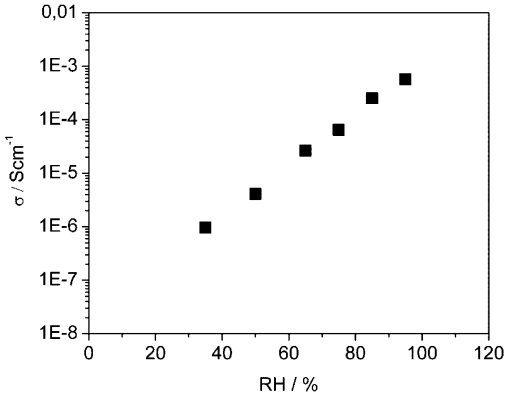

Figure 9. Conductivity of a ZPGly pellet as a function of RH at 100 °C.

For RH in the range 35−95%, the logarithm of the conductivity is a linear function of RH, and σ increases from 1.4×10^{-6} to 5.8×10^{-4} S cm^{-1}. As already observed for zirconium arylphosphonates,[2e] the strong conductivity dependence on RH is likely to be due to the weak acid character of the protogenic groups of ZPGly. It is interesting to observe that when the impedance data collected at different RH values are normalized by dividing Z' and Z'' by the pellet resistance (R) the points of the normalized Nyquist plots gather around the same semicircle (Figure 10).

This suggests that the pellet conductivity originates from only one type of proton transport because in general different types of transport (e.g., bulk, surface, or grain boundary transport) are expected to respond differently to RH changes, thus determining changes in the shape of the Nyquist plots as shown in ref 2j.

To get further insight into the physical origin of proton transport, water uptake determinations were carried out on pellets of ZPGly as a function of RH at 100 °C in the same RH range explored for conductivity measurements. The hydration of pellets (Figure 11) increases from ∼2 to 3 water molecules per unit formula for RH going from 35% to 95%, being always larger than the hydration of the material at room temperature. This is not surprising because, RH being the same, the water vapor pressure at 100 °C is by more than 40 times higher than that at 20 °C.

dx.doi.org/10.1021/ic502473w | Inorg. Chem. 2014, 53, 13220−13226

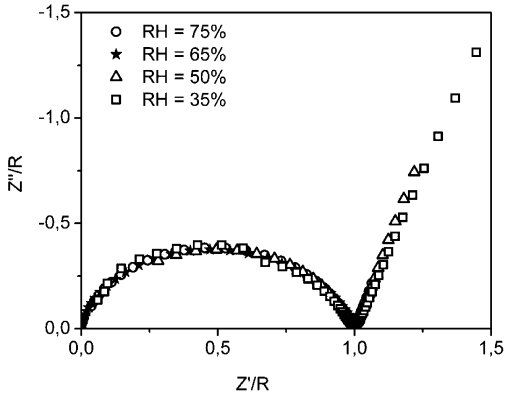

Figure 10. Normalized Nyquist plots at 100 °C and at the indicated RH values for a ZPGly pellet.

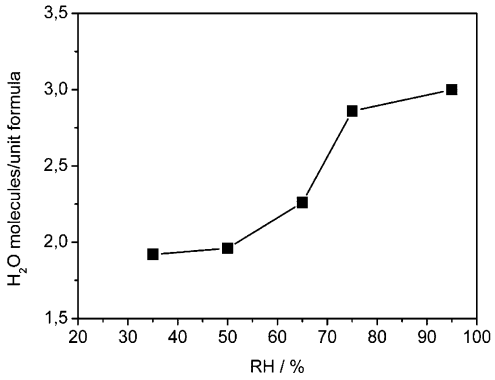

Figure 11. Hydration as a function of RH % at 100 °C for a ZPGly pellet.

Comparison of Figures 9 and 11 shows that in the RH range of 35−50% the conductivity increases by a factor of 3, while the hydration keeps nearly constant. Similarly, in the RH range of 75−95%, the conductivity increases by a factor of 9, while the hydration goes from 2.9 to 3 water molecules per unit formula. These findings suggest that the conductivity of ZPGly is not significantly affected by changes in the bulk hydration of ZPGly, but it reflects only the changes in the hydration of the surface of the ZPGly microcrystals. Therefore, in agreement with the invariance of the shape of the normalized Nyquist plots toward RH changes, it can be concluded that the conductivity of ZPGly pellets arises mainly from surface proton transport.

In comparison with other proton conducting systems with free acidic groups, ZPGly is less conductive than similar materials possessing sulfonic groups in the interlayer region, with σ as high as 0.07 S cm^{-1} at 100 °C/90% RH,[2h] probably due to the different acidic character of the protogenic groups. Finally, a straightforward comparison between the conductivity of ZPGly and that of most MOFs cannot be made due to the different experimental conditions of the measurements: high temperature/high RH for ZPGly, low temperature/high RH or high temperature/anhydrous conditions for MOFs. However, regardless of temperature and RH, the highest conductivity of ZPGly compares favorably with the best conductivity values reported for MOFs,[4a] which are on the order of 10^{-3} S cm^{-1}.

CONCLUSIONS

A novel layered zirconium phosphate diphosphonate with aminocarboxylic groups has been synthesized in mild condition. Due to the analogy of glyphosine and PMIDA moieties, the structure of this new compound shows some similarity with that of the previously reported ZPPMIDA: its layered nature and the presence of tetradentate phosphate and tridentate phosphonate groups with a similar structural role. However, the additional phosphonate group in glyphosine induces the presence of an increased number of P−O groups uncoordinated to metal atoms on the surface of layers, as compared to ZPPMIDA. These acidic groups, together with carboxylates, are responsible for the measured protonic conductivity. The conductivity behavior, studied as a function of temperature and relative humidity, and the concomitant determination of the hydration degree led to conclude that the conductivity is mainly due to surface proton transport. Future research will be addressed to the development of similar materials containing free acidic groups with an increased acidic strength in comparison with carboxylic groups, which could more efficiently enhance the proton transportation.

ASSOCIATED CONTENT

Supporting Information

Crystallographic information file and complete crystallographic parameters. PXRD patterns of ZPGly as synthesized and heated at 100 °C, Nyquist plots for ZPGly at 100 °C and different RH, Arrhenius plot of the conductivity for ZPGly pellet, PXRD patterns of ZPGly as synthesized, and after conductivity measurements. This material is available free of charge via the Internet at http://pubs.acs.org.

AUTHOR INFORMATION

Corresponding Author

*E-mail: riccardo.vivani@unipg.it.

Notes

The authors declare no competing financial interest.

ACKNOWLEDGMENTS

This work was supported by MIUR − Project FIRB 2010 no. RBFR10CWDA_003 and Fondazione Cassa di Risparmio di Perugia Project no. 2014.0100.021.

REFERENCES

(1) (a) Vivani, R.; Alberti, G.; Costantino, F.; Nocchetti, M. *Microporous Mesoporous Mater.* **2008**, *107*, 149−160. (b) Vivani, R.; Costantino, F.; Taddei, M. In *Metal Phosphonate Chemistry: From Synthesis to Applications*; Clearfield, A., Demadis, K., Eds.; RSC: Oxford, U.K., 2011; Chapter 2. (c) Clearfield, A.; Costantino, U. In *Comprehensive Supramolecular Chemistry*; Alberti, G., Bein, T., Eds.; Pergamon Press: Oxford, U.K., 1996; Vol. 7, p 107.

(2) (a) Alberti, G.; Costantino, U.; Casciola, M.; Vivani, R.; Peraio, A. *Solid State Ionics* **1991**, *46*, 61−68. (b) Alberti, G.; Casciola, M.; Costantino, U.; Peraio, A.; Montoneri, E. *Solid State Ionics* **1992**, *50*, 315−322. (c) Alberti, G.; Casciola, M.; Palombari, R.; Peraio, A. *Solid State Ionics* **1992**, *58*, 339−344. (d) Casciola, M.; Costantino, U.; Peraio, A.; Rega, T. *Solid State Ionics* **1995**, *77*, 229−233. (e) Alberti, G.; Boccali, L.; Casciola, M.; Massinelli, L.; Montoneri, E. *Solid State Ionics* **1996**, *84*, 97−104. (f) Alberti, G.; Costantino, U.; Casciola, M.; Ferroni, S.; Massinelli, L.; Staiti, P. *Solid State Ionics* **2001**, *145*, 249−255. (g) Casciola, M.; Alberti, G.; Ciarletta, A.; Cruccolini, A.; Piaggio, P.; Pica, M. *Solid State Ionics* **2005**, *176*, 2985−2989. (h) Alberti, G.; Casciola, M.; Donnadio, A.; Piaggio, P.; Pica, M.; Sisani, M. *Solid State Ionics* **2005**, *176*, 2893−2898. (i) Zima, V.; Svoboda, J.; Melanova, K.;

Benes, L.; Casciola, M.; Sganappa, M.; Brus, J.; Trchova, M. *Solid State Ionics* **2010**, *181*, 705−713. (j) Costantino, F.; Donnadio, A.; Casciola, M. *Inorg. Chem.* **2012**, *51*, 6992−7000.
(3) (a) Alberti, G.; Casciola, M. *Solid State Ionics* **2001**, *145*, 3−16. (b) Kreuer, K. D. *Chem. Mater.* **1996**, *8*, 610−641. (c) Colomban, P., Ed.; *Proton Conductors: Solids, Membranes and Gels Materials and Devices*; Cambridge University Press: Cambridge, U.K., 1992.
(4) (a) Yoon, M.; Suh, K.; Natarajan, S.; Kim, K. *Angew. Chem., Int. Ed.* **2013**, *52*, 2688−2700. (b) Taylor, J. M.; Dawson, K. W.; Shimizu, G. K. H. *J. Am. Chem. Soc.* **2013**, *135*, 1193−1196. (c) Bazaga-García, M.; Colodrero, R. M. P.; Papadaki, M.; Garczarek, P.; Zoń, J.; Olivera-Pastor, P.; Losilla, E. R.; León-Reina, L.; Aranda, M. A. G.; Choquesillo-Lazarte, D.; Demadis, K. D.; Cabeza, A. *J. Am. Chem. Soc.* **2014**, *136*, 5731−5739. (d) Colodrero, R. M. P.; Angeli, G. K.; Garcia, M. B.; Olivera-Pastor, P.; Villemin, D.; Losilla, E. R.; Martos, E. Q.; Hix, G. B.; Aranda, M. A. G.; Demadis, K. D.; Cabeza, A. *Inorg. Chem.* **2013**, *52*, 8770−8783. (e) Horike, S.; Umeyama, D.; Kitagawa, S. *Acc. Chem. Res.* **2013**, *46*, 2376−2384. (f) Zima, V.; Patil, D. S.; Raja, D. S.; Chang, T. G.; Lin, C. H.; Shimakawa, K.; Wagner, T. *J. Solid State Chem.* **2014**, *217*, 150−158.
(5) Taddei, M.; Donnadio, A.; Costantino, F.; Vivani, R.; Casciola, M. *Inorg. Chem.* **2013**, *52*, 12131−12139.
(6) (a) Poojary, D. M.; Zhang, B.; Clearfield, A. *Angew. Chem., Int. Ed.* **1994**, *33*, 2324−2326. (b) Zhang, B.; Poojary, D. M.; Clearfield, A.; Peng, G.-Z. *Chem. Mater.* **1996**, *8*, 1333−1340.
(7) Moedritzer, K.; Irani, R. R. *J. Org. Chem.* **1966**, *31*, 1603−1607.
(8) Favre-Nicolin, V.; Cerny, R. *J. Appl. Crystallogr.* **2002**, *35*, 734−743.
(9) (a) Werner, P. E.; Eriksson, L.; Westdhal, M. *J. Appl. Crystallogr.* **1985**, *18*, 367−370. (b) Boultif, A.; Louer, D. *J. Appl. Crystallogr.* **2004**, *37*, 724−731.
(10) Larson, C.; von Dreele, R. B. *Generalized Crystal Structure Analysis System*; Los Alamos National Laboratory: Los Alamos, NM, 2001.
(11) (a) Taddei, M.; Costantino, F.; Manuali, V.; Vivani, R. *Inorg. Chem.* **2011**, *50*, 10835−10843. (b) Costantino, F.; Sassi, P.; Geppi, M.; Taddei, M. *Cryst. Growth Des.* **2012**, *12*, 5462−5470.
(12) (a) Costantino, U.; Nocchetti, M.; Vivani, R. *J. Am. Chem. Soc.* **2002**, *124*, 8428−8434. (b) Vivani, R.; Costantino, F.; Nocchetti, M.; Gatta, G. D. *J. Solid State Chem.* **2004**, *177*, 4013−4018.